CFD Letters

Journal homepage:
https://semarakilmu.com.my/journals/index.php/CFD_Letters/index
ISSN: 2180-1363

Analysis of Blood Flow in Human Brain Vessels for Newtonian and Non-Newtonian Blood Properties

Nayeem Imtiaz[1,*], Tasfia Siam[2]

[1] Kate Gleason College of Engineering, Rochester Institute of Technology, Rochester, NY 14623, USA
[2] Shaheed Tajuddin Ahmad Medical College Hospital, Gazipur 1712, Bangladesh

ARTICLE INFO

Article history:
Received 13 February 2023
Received in revised form 10 March 2023
Accepted 11 April 2023
Available online 1 September 2023

Keywords:
Brain MRI; vertebral-basilar artery; non-Newtonian blood

ABSTRACT

The cerebral artery system can be affected by various diseases such as stroke, carotid stenosis, vertebral stenosis, intracranial stenosis, aneurysms, and vascular malformations. Understanding the blood flow specific to each patient's cerebral arteries can provide crucial information about how these diseases progress and guide potential treatment options. A patient-specific Magnetic Resonance Imaging (MRI) scan of a human brain was utilized to create a 3D model of the arterial system. Blood flow simulations were conducted using the ANSYS (Fluent) R2021 software package. The ICEM meshing tool within the ANSYS software was employed to prepare the models. The velocity rise and pressure drop were observed in the branching of the basilar artery. This can provide valuable patient specific information on various cerebral diseases, and drug delivery cases. The non-Newtonian properties of blood were established by inputting the Power Law parameters into the ANSYS Fluent system. It was observed that the effects of non-Newtonian properties of blood are relatively negligible for the large vessels studied (> 200 um).

1. Introduction

Mathematical modelling has emerged as a valuable tool for researchers to investigate and analyze a wide range of blood flow conditions in the human body using computational methods [1-4]. The primary objective of these studies is to enhance our understanding of the propagation of diseases and facilitate the discovery of new drugs [5,6]. By utilizing mathematical models, researchers can simulate complex physiological processes and investigate how various factors affect blood flow, enabling them to make accurate predictions and test different hypotheses [7-10]. These studies have the potential to significantly advance our understanding of the human body and pave the way for more effective treatments for a range of medical conditions.

During the past decade, the computational analysis of blood flow in human arteries has been elaborately studied [11-16]. CFD helps researchers analyze blood flow conditions inside complex artery systems, that are highly difficult to analyze empirically. One of the most critical and complex artery systems is the cerebral artery [17]. Diseases that may take place in the cerebral artery system

* *Corresponding author.*
E-mail address: ni2631l@rit.edu (Nayeem Imtiaz)

https://doi.org/10.37934/cfdl.15.9.4555

include stroke, carotid stenosis, vertebral stenosis, intracranial stenosis, aneurysms, and vascular malformations [18]. Gaining knowledge on patient-specific blood flow through the cerebral arteries will provide valuable insight into the mentioned disease propagation and possible treatment steps.

The method to incorporate a PC-MRI signal model into a Newtonian fluid computational model was proposed by Rispoli *et al.*, [19] where the researchers studied fluid flow in a carotid bifurcation. Another study performed by Gharahi *et al.,* [20] introduced a computational model that studied carotid bifurcation based on actual human anatomy and volumetric flow rate obtained by PC-MRI data. They found that the PC-MRI data outputted non-precise results when measuring the blood velocity near the artery walls, whereas Computational Fluid Dynamics (CFD) on the other hand provided more accurate results. Furthermore, various mathematical modeling studies have been performed where the non-Newtonian properties of blood have been explored. For example, Priyadharsini *et al.,* [21] performed a study on blood viscosity changes based on body thermoregulatory responses in a stretched capillary. Krishna *et al.,* [22] proposed a continuum model for the transport of red blood cells (RBC) inside arteries and capillaries of small diameters. Haipeng *et al.,* [23] aimed to investigate the differences in cerebral hemodynamic metrics built with Newtonian and non-Newtonian fluid assumptions, in patients with intracranial atherosclerotic stenosis.

Although there have been numerous CFD studies that involve a non-Newtonian model of blood, the study that incorporates a patient-specific non-Newtonian blood flow model in a human cerebral basilar artery has not been widely studied [24-27]. A non-Newtonian fluid is a fluid that has viscosity changes with applied shear. Blood is a shear-thinning fluid, which means the viscosity decreases with increased shear [28-30]. On the other hand, a Newtonian fluid is a fluid that has constant viscosity with applied shear. A patient-specific CFD model that is incorporated with the non-Newtonian properties of blood, can be a suitable platform to broaden the understanding of cerebrovascular diseases.

This study focuses on simulating and comparing Newtonian and non-Newtonian blood flow properties inside a patient-specific anatomically accurate vertebral-basilar artery system (an artery within the cerebral system) (Figure 1). The aim of this report is to study hemodynamic parameters (velocity & pressure) inside the arterial system of interest. The model includes the vertebral artery, basilar artery, and posterior cerebral artery.

An actual MRI of a human brain was considered for obtaining the 3D model of the arterial system. ANSYS (Fluent) R2021 software package was used to perform the simulations. The meshing tool ICEM within the ANSYS software system was used to perform the meshing of the models. The non-Newtonian properties of blood were established by inputting the Power Law parameters in the ANSYS Fluent system.

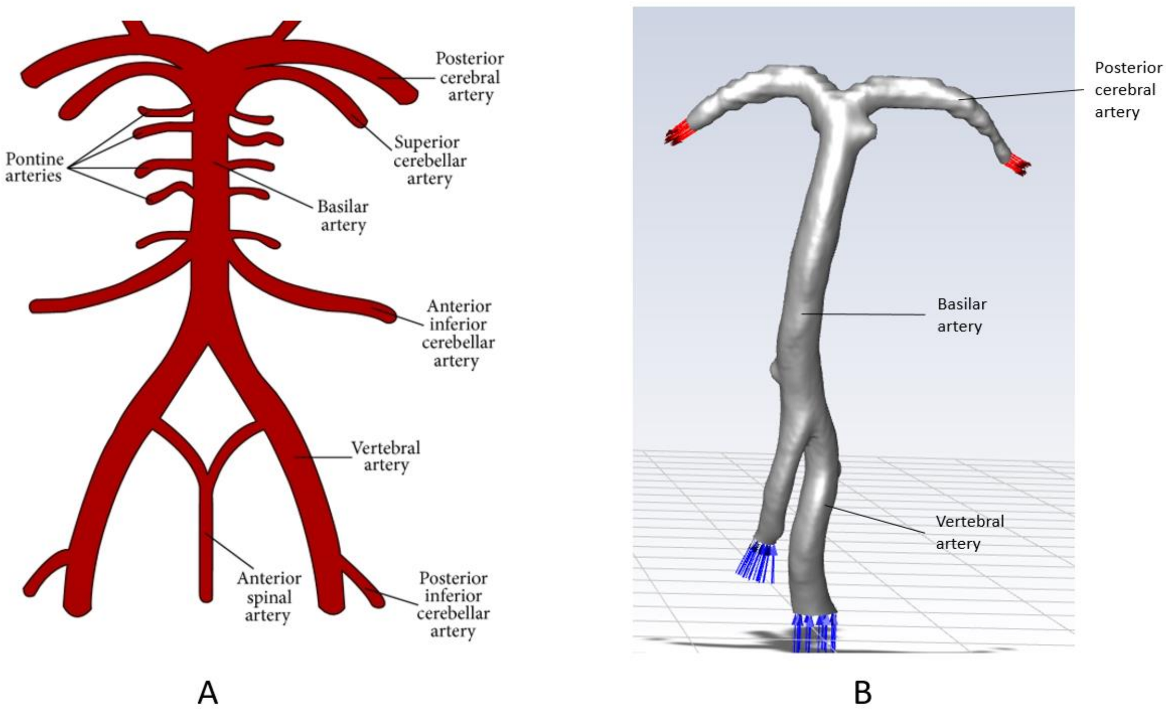

Fig. 1. A) Vertebral-basilar artery system [31], B) 3D model of the vertebral-basilar artery considered for simulation.

2. Material and Methods

In Figure 1A, we can see the Vertebral-basilar artery system. The cerebral arteries are responsible for supplying blood to different regions of the brain and adjacent structures. The largest of these arteries is the middle cerebral artery, which provides blood to the lateral surface of each hemisphere. In contrast, the anterior cerebral artery supplies blood to the medial surface of the brain, while the ophthalmic artery supplies blood to the eye and related facial structures. At the level of the brainstem, the two vertebral arteries merge to form the basilar artery, which supplies blood to the posterior part of the cerebral hemispheres, including the occipital and posterior temporal lobes, the cerebellum, and the brainstem. This is also known as vertebrobasilar or posterior circulation [31].

MRIcroGL, VMTK, Paraview, and Meshmixer softwares were used to get from an actual human brain MRI scan to an isolated blood vessel for simulation. An actual human brain MRI Dicom file was opened using the MRIcroGL software. The dicom file was converted to nii format using a tool within the MRIcroGL software. Then the nii file was opened in VMTK and converted to vti format. The vti file was opened using the Paraview software and the vessel section of interest was isolated. The isolated vessels were opened again in VMTK software for iso-surface selection and was saved in stl format. Iso-surface parameter of 100 was selected for this study. The stl files were opened in Meshmixer to further isolate the blood vessels. The Vertebral-basilar artery was isolated in Meshmixer and the inlets and outlets were demarcated. The final 3D geometry was exported as an stl part file. The workflow process of achieving a 3D geometry from an actual human MRI is shown in Figure 2. The geometrical features of the 3D model of the cerebral artery are shown in Table 1.

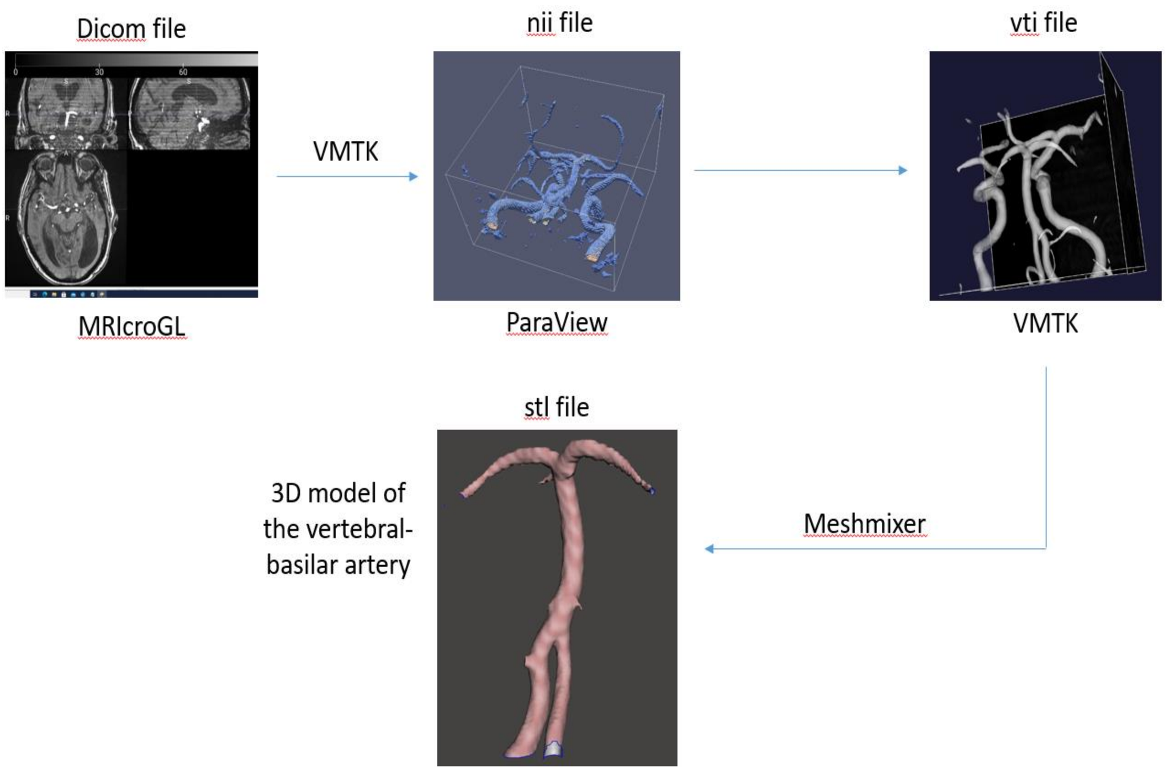

Fig. 2. Workflow to obtain stl 3D geometry from Dicom MRI file.

Table 1
Geometrical features of the Vertebral-basilar artery system

Vertebral-Basilar Artery Length (mm): 16.87				
Measurements of Interest	Vertebral Artery		Posterior Cerebral Artery	
	Large Inlet	Small Inlet	Large Outlet	Small Outlet
Lumen dia (mm)	6	4	4.5	1.62
Arm Length	-	-	13.6	16

The numerical workflow of performing the CFD analysis is shown in the flow chart in Figure 3. The 3D geometry obtained from Meshmixer was used to generate the mesh. Suitable physics models for Newtonian and non-Newtonian blood were set up in ANSYS Fluent and calculations were run (more descriptions on each step have been provided later). The simulation results were cross-examined by manual calculations and validation of the non-Newtonian flow model was provided.

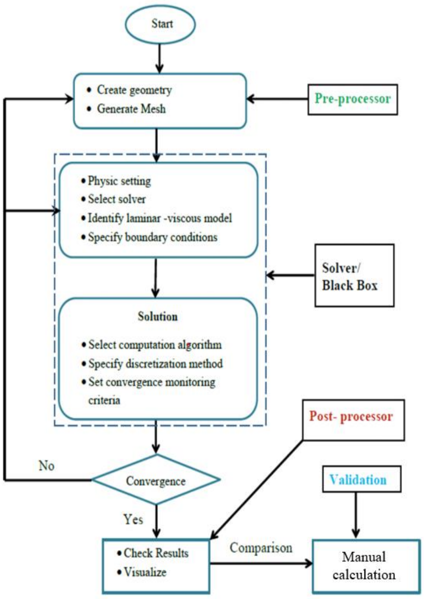

Fig. 3. Numerical methodology flow chart for fluent simulation [32]

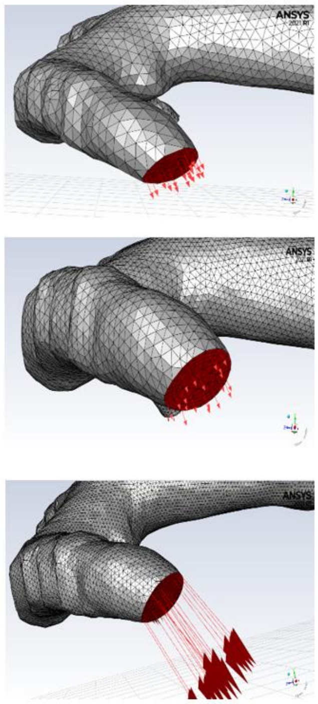

Fig. 4. Progression of mesh sizes: coarse to fine

ICEM tool was used to generate three different sizes of mesh. The minimum mesh element sizes selected for the model were 0.2 mm, 0.3 mm, and 0.5 mm respectively. Three layers of mesh were generated for vessel walls to obtain a well-defined fluid boundary layer in the interior walls. For the different mesh sizes 0.2, 0.3, and 0.5, numbers of generated elements were 1.4 M, 0.42 M, and 97 K respectively. Figure 4 shows the different types of the generated mesh.

In the setup section of Fluent the inlet temperatures were set as 310 K (normal temperature of human blood). The heat transfer energy equation was incorporated in the setup (Eq. (1)) [33]. In Eq. (1) k_{eff} is the effective conductivity ($k + k_t$, where k_t is the turbulent thermal conductivity, defined by the active turbulence model), and $\vec{J}_j$ is the diffusion flux of species *j*. In Eq. (1), the right-hand side includes three terms that represent how energy is transferred in the system. The first term is related to conduction, the second term is related to the diffusion of species, and the third term is related to viscous dissipation. S_h includes the heat of chemical reaction. The inlet of the small vertebral artery blood velocity was set to 0.32 m/s and the large one was set to 0.3 m/s, assuming a total blood flow through the cerebral artery to be 750 ml/min (normal range in healthy adults) [34]. For fluid flow through the artery, Fluent solves the Navier-Stokes continuity equation and the equation of motion (Eq. (2), Eq. (3) respectively) [35]. The continuity equation (Eq. (2)) states that the rate of change of mass in a given volume of fluid is equal to the net rate of mass flow into or out of that volume. In other words, it says that mass cannot be created or destroyed, only redistributed within the fluid. The equation of motion or momentum equation (Eq. (3)) states that the rate of change of momentum in a given volume of fluid is equal to the net rate of momentum flow into or out of that volume, plus the net force acting on the fluid. In other words, it says that momentum cannot be created or destroyed, only redistributed within the fluid.

$$\frac{\partial}{\partial t}(\rho E) + \nabla.\left(\vec{v}(\rho E + p)\right) = \nabla.\left(k_{eff}\nabla T - \sum_j h_j \vec{J}_j + \left(\bar{\bar{T}}_{eff}.\vec{v}\right)\right) + S_h \tag{1}$$

$$\nabla.\vec{u} = 0 \tag{2}$$

$$\rho\left(\frac{\partial \vec{u}}{\partial t} + (\vec{u}.\nabla)\vec{u}\right) = -\nabla p + \mu\nabla^2\vec{u} + \rho\vec{F} \tag{3}$$

A custom input was provided in the material section to create Newtonian blood. The density, specific heat, thermal conductivity, and viscosity of the blood was set to be 1060 [kg/m^3], 3513 [J/ Kg-K], 0.44 [W/ m-K], and 0.003 [kg/ m-s] respectively [36]. To create non-Newtonian blood the "turbulence- expert" was activated in the Fluent console window and the option "non-Newtonian Power Law" was selected for viscosity. The Power Law parameters for the consistency index k, power law index n, minimum viscosity limit, and maximum viscosity limit were selected to be 0.2073 [kg sn-2m-1], 0.4851, 0.00125 [kg/ m-s], and 0.003 [kg/ m-s] respectively. These parameters were based on previously published literature [37,38]. The convergence tolerance was set to 1e-6 for the calculations. 200 iterations of calculation were performed per simulation case. The vessel wall material was selected as Aluminium and the blood velocity along the vessel was set to be zero. The reason is, as the bulk of the blood flow happens within the vessel wall due to arterial blood pressure (lies between 60 and 80 mmHg) [39], the flow induced by vessel wall permeability is negligible [40].

To validate the obtained simulation results some manual calculations were performed for the small outlet and large inlet velocity and pressure using the volume flow rate equation (Eq. (4)) and Bernoulli's equation (Eq. (5)). In Eq. (4), *Q* is the flow rate, *A* cross-sectional area of the artery, and *V* the blood velocity within the artery. In Eq. (5), P_1, v_1, and h_1 are the vessel inlet blood pressure, velocity, and height respectively and P_2, v_2, and h_2 are the vessel outlet blood pressure, velocity, and height respectively.

$$Q = A.V \tag{4}$$

$$P_1 + \frac{1}{2}\rho v_1^2 + \rho g h_1 = P_2 + \frac{1}{2}\rho v_2^2 + \rho g h_2 \tag{5}$$

3. Results and Discussion

The simulation results have been summarized in Table 2. It was observed that for all the mesh conditions the velocity and pressure results were in a similar range, meaning the model is mesh-independent to an acceptable degree. Thus, just one mesh size (0.3 mm) was considered for non-Newtonian flow analysis. Figure 5. shows how the velocity has a spike near the outlet of the artery and the pressure has a sudden drop (velocities and pressures were calculated along the X-axis: length of the Basilar). Due to the small outlet lumen, this abrupt velocity and pressure change were observed. The pressure drops to zero in the outlet as the blood escapes the vessel enclosure. However, this pressure drop to zero is due to considering the artery is sectioned off from the full cerebral artery systems. In actual human brain anatomy the basilar-artery branches into smaller sections, and morphs into capillaries, distributing the flow and pressure. So our model gives valuable pressure and velocity information within the vessel system, and the values at the outlet are not of consideration. From, Figures 5A and 5B we can see how the velocity increases and the pressure drops when the basilar-artery branches into two posterior cerebral arteries. In Figure 5, the branching happens when the X-axis point is at -60 m (position along the artery length). At that point, the velocity of the blood increases 7X (0.5 m/s to 3.5 m/s) and almost a 7000 Pa pressure drop occurs. This sudden change in velocity and pressure in the branching can be a key factor in studying the cerebral aneurysm that occurs near the branch [41].

Figure 6 shows the contour, vector, and streamline plots for the velocity and pressure. Assuming the blood flow rate through the small outlet to be 300 ml/min the calculated velocity using Eq. (4) was seen to be 2.4 m/s and the large inlet pressure was calculated to be 2290 Pa (using Eq. (5)). Figure 6A, 6B, and 6B show the velocity contours, velocity streamlines, and velocity vectors of the blood within the vessel respectively. This can provide valuable information on patient-specific targeted drug delivery and drug discovery studies. Figure 6D shows the local static pressure regions within the vessel. It is possible that this information can offer personalized data to identify the exact point within a blood vessel that may be at the greatest risk for cerebral hemorrhage.

Table 2
Result Summary

		Inlet-large		Inlet-small		Outlet-large		Outlet-small	
Mesh (mm)	Blood Property	Pr. (Pa)	V (m/s)	Pr. (Pa)	V (m/s)	Pr. (Pa)	V (m/s)	Pr. (Pa)	V (m/s)
0.3	Newtonian	2725	0.3	2925	0.32	0	1.71	0	2.02
0.2	Newtonian	2550	0.3	2720	0.32	0	1.69	0	2.06
0.5	Newtonian	2800	0.3	3130	0.32	0	1.773	0	2.25
0.3	Non- Newtonian	2650	0.3	2820	0.32	0	1.725	0	2.11

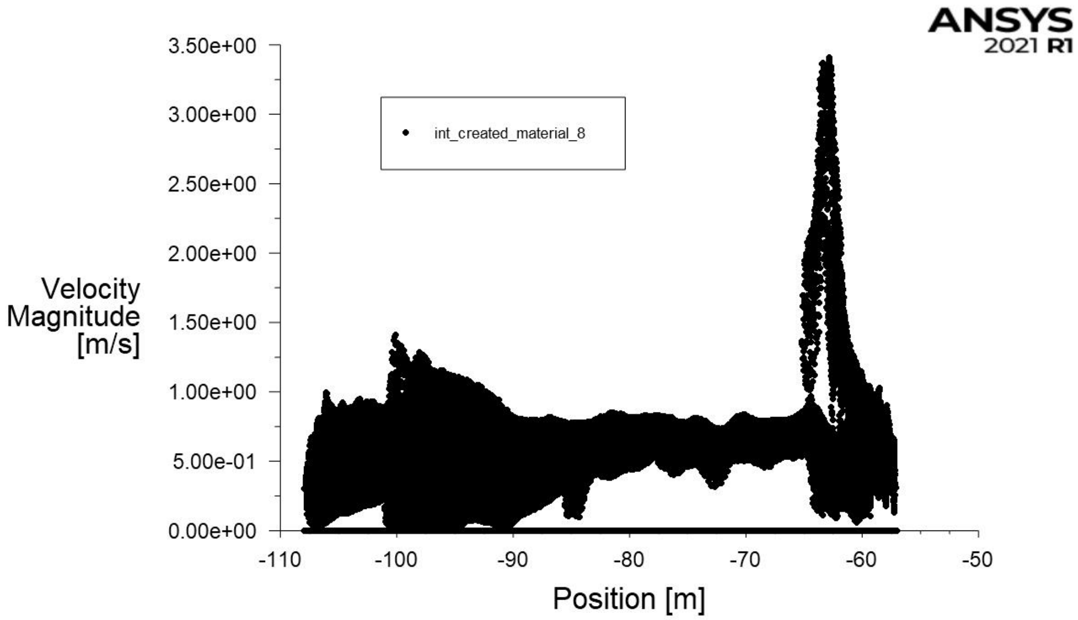

A

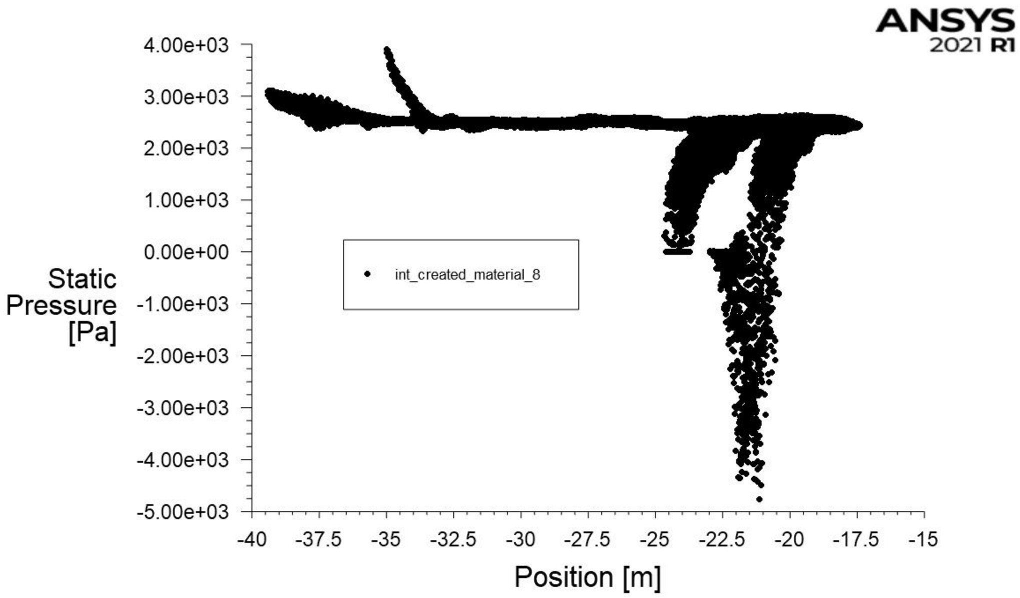

B

Fig. 5. A) Velocity magnitude rises near the exit of the vessel, B) static pressure drops near the exit of the vessel

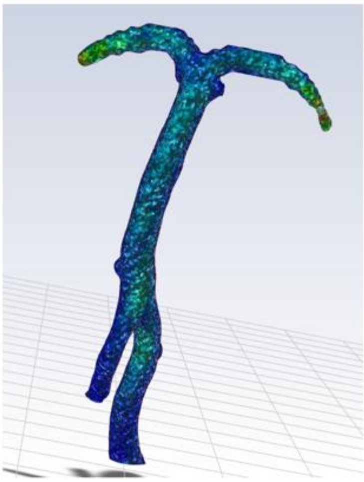

A

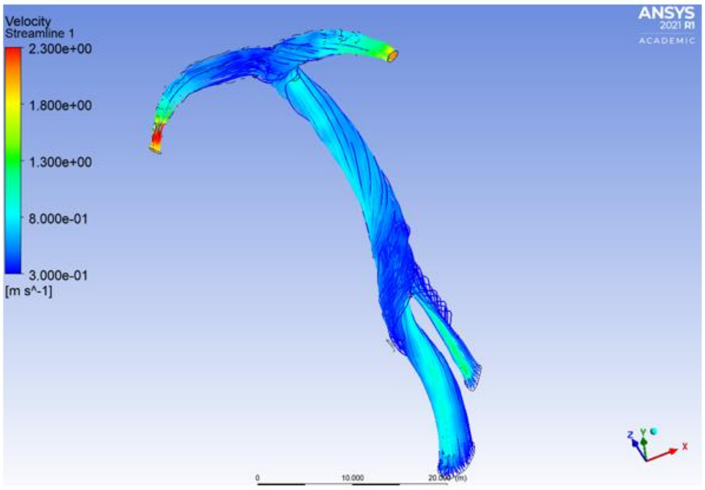

B

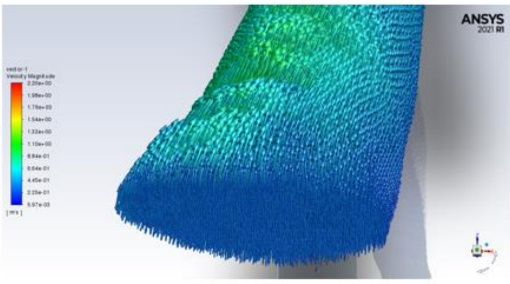

C

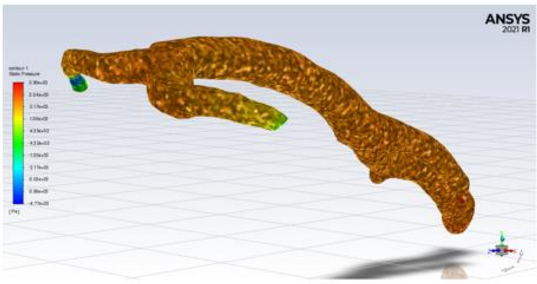

D

Fig. 6. A) Velocity contour, B) velocity streamlines that the blood particles follow, c) velocity vectors at the large inlet, D) static pressure contours.

It was observed that setting blood as a non-Newtonian fluid did not significantly change the velocity and pressure values as found for Newtonian blood. This might happen due to the fact that, non-Newtonian properties of blood are significantly apparent for microcirculation i.e. for very small vessel diameters (< 200 um). As the minimum lumen diameter this study dealt with was around 1.5 mm, the non-Newtonian properties of blood did not factor in. It was also observed that the calculated velocity at the outlet was within 19% of the simulations, and the pressure at the large inlet was within 16% of the simulations. These discrepancies may have occurred due to not considering the gravitational effects of fluid and the un-uniform nature of the blood vessel inlet in the manual calculations.

4. Conclusions

The effects of non-Newtonian properties of blood are relatively negligible for large vessels (> 200 um). The simulations were within a tolerable percentage of the manual calculations (~15%). The 3D geometry of the Vertebral-basilar artery was mesh independent to an acceptable degree. Although the simulations were not verified using PC-MRI data, the simulation models provided in this study can be used to analyze the effect of blood flow patterns for complex disease conditions, such as the development of a cerebral aneurysm. Also, the model can potentially analyze cerebral drug delivery using blood as the medium. The patient-specific computational simulation can also provide valuable information on targeted drug delivery and drug discovery studies.

Future work could include the study of non-Newtonian blood flow for microcirculation through capillaries, to incorporate pulsatile flow behaviors in the model, to see how blood behaves when subjected to blood thinners (i.e. Heparin), etc. A potential future work could be to incorporate dynamic meshing and boundary conditions suitable to analyze the effects of vascular resistance and vessel compliance on fluid dynamics.

Acknowledgment
This research was not funded by any grant.

References

[1] Mahrous, Samar Ahmed, Nor Azwadi Che Sidik, and Khalid Mansour Saqr. "Investigation of Newtonian and Power-Law Blood Flow Models in a 180 Curved Pipe at Low to Medium Shear Rate." *Journal of Advanced Research in Fluid Mechanics and Thermal Sciences* 69, no. 1 (2020): 148-162. https://doi.org/10.37934/arfmts.69.1.148162

[2] Ramdan, Salman Aslam, Mohammad Rasidi Rasani, Thinesh Subramaniam, Ahmad Sobri Muda, Ahmad Fazli Abdul Aziz, Tuan Mohammad Yusoff Shah Tuan Ya, Hazim Moria, Mohd Faizal Mat Tahir, and Mohd Zaki Nuawi. "Blood Flow Acoustics in Carotid Artery." *Journal of Advanced Research in Fluid Mechanics and Thermal Sciences* 94, no. 1 (2022): 28-44. https://doi.org/10.37934/arfmts.94.1.2844

[3] Ningappa, Abhilash Hebbandi, Suraj Patil, Gowrava Shenoy Belur, Augustine Benjamin Valerian Barboza, Nitesh Kumar, Raghuvir Pai Ballambat, Adi Azriff Basri, Shah Mohammed Abdul Khader, and Masaaki Tamagawa. "Influence of altered pressures on flow dynamics in carotid bifurcation system using numerical methods." *Journal of Advanced Research in Fluid Mechanics and Thermal Sciences* 97, no. 1 (2022): 47-61. https://doi.org/10.37934/arfmts.97.1.4761

[4] Zin, Ahmad Faiz Mat, Ishkrizat Taib, Muhammad Hanafi Asril Rajo Mantari, Bukhari Manshoor, Ahmad Mubarak Tajul Arifin, Mahmod Abd Hakim Mohamad, Muhammad Sufi Roslan, and Muhammad Rafiuddin Azman. "Temperature Variation with Hemodynamic Effect Simulation on Wall Shear Stress in Fusiform Cerebral Aneurysm." *Journal of Advanced Research in Fluid Mechanics and Thermal Sciences* 95, no. 2 (2022): 40-54.

[5] Zain, Norliza Mohd, Zuhaila Ismail, and Peter Johnston. "A Stabilized Finite Element Formulation of Non-Newtonian Fluid Model of Blood Flow in A Bifurcated Channel with Overlapping Stenosis." *Journal of Advanced Research in Fluid Mechanics and Thermal Sciences* 88, no. 1 (2021): 126-139. https://doi.org/10.37934/arfmts.88.1.126139

[6] Chen, Aolin, Adi Azriff Basri, Norzian Ismail, Di Zhu, and Kamarul Arifin Ahmad. "Numerical Study of Subaortic Stenosis and Pannus Formation on Blood Flow Around Mechanical Heart Valves." *Journal of Advanced Research in Fluid Mechanics and Thermal Sciences* 95, no. 2 (2022): 180-190.

[7] Zakaria, Mohamad Shukri, Siti Hajar Zainudin, Haslina Abdullah, Cheng See Yuan, Mohd Juzaila Abd Latif, and Kahar Osman. "CFD Simulation of Non-Newtonian Effect on Hemodynamics Characteristics of Blood Flow through Benchmark Nozzle." *Journal of Advanced Research in Fluid Mechanics and Thermal Sciences* 64, no. 1 (2019): 117-125.

[8] Imtiaz, Nayeem, William A. Stoddard, Arthur T. Johnson, Corrine R. Amato, Jared A. Carter, James A. Roussie, and Steven W. Day. "PULM7: Development of a Miniaturized ECMO Device on a Microfluidic Platform." *ASAIO Journal* 68, no. Supplement 2 (2022): 87. https://doi.org/10.1097/01.mat.0000841196.95976.61

[9] Hegde, Pranav, SM Abdul Khader, Raghuvir Pai, Masaaki Tamagawa, Ravindra Prabhu, Nitesh Kumar, and Kamarul Arifin Ahmad. "CFD Analysis on Effect of Angulation in A Healthy Abdominal Aorta-Renal Artery Junction." *Journal of Advanced Research in Fluid Mechanics and Thermal Sciences* 88, no. 1 (2021): 149-165. https://doi.org/10.37934/arfmts.88.1.149165

[10] Zain, Norliza Mohd, and Zuhaila Ismail. "Dynamic Response of Heat Transfer in Magnetohydrodynamic Blood Flow Through a Porous Bifurcated Artery with Overlapping Stenosis." *Journal of Advanced Research in Fluid Mechanics and Thermal Sciences* 101, no. 1 (2023): 215-235. https://doi.org/10.37934/arfmts.101.1.215235

[11] Wahyudi, Slamet, Nanda Raihan Vardiansyah, and Putu Hadi Setyorini. "Effect of Blood Perfusion on Temperature Distribution in the Multilayer of the Human Body with Interstitial Hyperthermia Treatment for Tumour Therapy." *CFD Letters* 14, no. 6 (2022): 102-114. https://doi.org/10.37934/cfdl.14.6.102114

[12] Zain, Norliza Mohd, Zuhaila Ismail, and Peter Johnston. "Numerical Analysis of Blood Flow Behaviour in a Constricted Porous Bifurcated Artery under the Influence of Magnetic Field." *CFD Letters* 15, no. 1 (2023): 39-58. https://doi.org/10.37934/cfdl.15.1.3958

[13] Saufi, Ommar Mykael Mat, Nur Amani Hanis Binti Roseman, Ishkrizat Taib, Nurul Fitriah Nasir, Ahmad Mubarak Tajul Ariffin, Nor Adrian Nor Salim, Shahrul Azmir Osman, Nofrizal Idris Darlis, and Ali Kamil Kareem. "Flow Characteristics on Carotid Artery Bifurcation of Different Aneurysmal Morphology." *CFD Letters* 15, no. 2 (2023): 25-40. https://doi.org/10.37934/cfdl.15.2.2540

[14] Alastruey, Jordi, Nan Xiao, Henry Fok, Tobias Schaeffter, and C. Alberto Figueroa. "On the impact of modelling assumptions in multi-scale, subject-specific models of aortic haemodynamics." *Journal of The Royal Society Interface* 13, no. 119 (2016): 20160073. https://doi.org/10.1098/rsif.2016.0073

[15] Lopes, D., Hélder Puga, J. Carlos Teixeira, and S. F. Teixeira. "Influence of arterial mechanical properties on carotid blood flow: Comparison of CFD and FSI studies." *International Journal of Mechanical Sciences* 160 (2019): 209-218. https://doi.org/10.1016/j.ijmecsci.2019.06.029

[16] Jin, Zan-Hui, M. Barzegar Gerdroodbary, P. Valipour, M. Faraji, and Nidal H. Abu-Hamdeh. "CFD investigations of the blood hemodynamic inside internal cerebral aneurysm (ICA) in the existence of coiling embolism." *Alexandria Engineering Journal* 66 (2023): 797-809. https://doi.org/10.1016/j.aej.2022.10.070

[17] Lee, Robert MKW. "Morphology of cerebral arteries." *Pharmacology & therapeutics* 66, no. 1 (1995): 149-173. https://doi.org/10.1016/0163-7258(94)00071-A

[18] Portegies, M. L. P., P. J. Koudstaal, and M. A. Ikram. "Cerebrovascular disease." *Handbook of clinical neurology* 138 (2016): 239-261. https://doi.org/10.1016/B978-0-12-802973-2.00014-8

[19] Mittal, Rajat, Jung Hee Seo, Vijay Vedula, Young J. Choi, Hang Liu, H. Howie Huang, Saurabh Jain, Laurent Younes, Theodore Abraham, and Richard T. George. "Computational modeling of cardiac hemodynamics: Current status and future outlook." *Journal of Computational Physics* 305 (2016): 1065-1082. https://doi.org/10.1016/j.jcp.2015.11.022

[20] Gharahi, Hamidreza, Byron A. Zambrano, David C. Zhu, J. Kevin DeMarco, and Seungik Baek. "Computational fluid dynamic simulation of human carotid artery bifurcation based on anatomy and volumetric blood flow rate measured with magnetic resonance imaging." *International journal of advances in engineering sciences and applied mathematics* 8 (2016): 46-60. https://doi.org/10.1007/s12572-016-0161-6

[21] Priyadharsini, M. "Mathematical modelling and analysis of thermoregulation effects on blood viscosity under magnetic effects and thermal radiation in a permeable stretching capillary." *Journal of Thermal Biology* 111 (2023): 103398. https://doi.org/10.1016/j.jtherbio.2022.103398

[22] Chandran, Krishna, Indranil Saha Dalal, Kazuya Tatsumi, and Krishnamurthy Muralidhar. "Numerical simulation of blood flow modeled as a fluid-particulate mixture." *Journal of Non-Newtonian Fluid Mechanics* 285 (2020): 104383. https://doi.org/10.1016/j.jnnfm.2020.104383

[23] Liu, Haipeng, Linfang Lan, Jill Abrigo, Hing Lung Ip, Yannie Soo, Dingchang Zheng, Ka Sing Wong et al. "Comparison of Newtonian and non-Newtonian fluid models in blood flow simulation in patients with intracranial arterial stenosis." *Frontiers in physiology* 12 (2021): 718540. https://doi.org/10.3389/fphys.2021.782647

[24] Chan, Weng Yew, Yan Ding, and J. Y. Tu. "Modeling of non-Newtonian blood flow through a stenosed artery incorporating fluid-structure interaction." *Anziam Journal* 47 (2005): C507-C523. https://doi.org/10.21914/anziamj.v47i0.1059

[25] Mohd Adib, Mohd Azrul Hisham, Satoshi Ii, Yoshiyuki Watanabe, and Shigeo Wada. "Minimizing the blood velocity differences between phase-contrast magnetic resonance imaging and computational fluid dynamics simulation in cerebral arteries and aneurysms." *Medical & biological engineering & computing* 55 (2017): 1605-1619. https://doi.org/10.1007/s11517-017-1617-y

[26] Liu, Jia, Zhengzheng Yan, Yuehua Pu, Wen-Shin Shiu, Jianhuang Wu, Rongliang Chen, Xinyi Leng et al. "Functional assessment of cerebral artery stenosis: a pilot study based on computational fluid dynamics." *Journal of Cerebral Blood Flow & Metabolism* 37, no. 7 (2017): 2567-2576. https://doi.org/10.1177/0271678X16671321

[27] Jamali, Muhammad Sabaruddin Ahmad, Zuhaila Ismail, and Norsarahaida Saidina Amin. "Effect of Different Types of Stenosis on Generalized Power Law Model of Blood Flow in a Bifurcated Artery." *Journal of Advanced Research in Fluid Mechanics and Thermal Sciences* 87, no. 3 (2021): 172-183. https://doi.org/10.37934/arfmts.87.3.172183

[28] Bodnár, Tomás, Adélia Sequeira, and M. Prosi. "On the shear-thinning and viscoelastic effects of blood flow under various flow rates." *Applied Mathematics and Computation* 217, no. 11 (2011): 5055-5067. https://doi.org/10.1016/j.amc.2010.07.054

[29] Lanotte, Luca, Johannes Mauer, Simon Mendez, Dmitry A. Fedosov, Jean-Marc Fromental, Viviana Claveria, Franck Nicoud, Gerhard Gompper, and Manouk Abkarian. "Red cells' dynamic morphologies govern blood shear thinning under microcirculatory flow conditions." *Proceedings of the National Academy of Sciences* 113, no. 47 (2016): 13289-13294. https://doi.org/10.1073/pnas.1608074113

[30] Anand, M., and K. R. Rajagopal. "A shear-thinning viscoelastic fluid model for describing the flow of blood." *International Journal of Cardiovascular Medicine and Science* 4, no. 2 (2004): 59-68.

[31] Flanagan, Michael F. "The role of the craniocervical junction in craniospinal hydrodynamics and neurodegenerative conditions." *Neurology Research International* 2015 (2015). https://doi.org/10.1155/2015/794829

[32] Muiruri, Patrick Irungu, and Oboetswe Seraga Motsamai. "Three Dimensional CFD Simulations of A Wind Turbine Blade Section; Validation." *Journal of Engineering Science & Technology Review* 11, no. 1 (2018). https://doi.org/10.25103/jestr.111.16

[33] Manual, U. D. F. "ANSYS FLUENT 12.0." *Theory Guide* (2009): 67.

[34] Siesjö, Bo K. "Cerebral circulation and metabolism." *Journal of neurosurgery* 60, no. 5 (1984): 883-908. https://doi.org/10.3171/jns.1984.60.5.0883

[35] Constantin, Peter, and Ciprian Foias. Navier-stokes equations. University of Chicago Press, 2020.

[36] Faber, James E., and George A. Stouffer. "Introduction to basic hemodynamic principles." *Cardiovascular hemodynamics for the clinician* (2017): 1-16. https://doi.org/10.1002/9781119066491.ch1

[37] Hussain, Mohammad A., Subir Kar, and Ram R. Puniyani. "Relationship between power law coefficients and major blood constituents affecting the whole blood viscosity." *Journal of Biosciences* 24 (1999): 329-337. https://doi.org/10.1007/BF02941247

[38] Hussain, A., R. R. Puniyani, and S. Kar. "Quantification of blood viscosity using power law model in cerebrovascular accidents and high risk controls." *Clinical Hemorheology and Microcirculation* 14, no. 5 (1994): 685-696. https://doi.org/10.3233/CH-1994-14507

[39] Rosner, Michael J., Sheila D. Rosner, and Alice H. Johnson. "Cerebral perfusion pressure: management protocol and clinical results." *Journal of neurosurgery* 83, no. 6 (1995): 949-962. https://doi.org/10.3171/jns.1995.83.6.0949

[40] Raichle, Marcus E., Boyd K. Hartman, John O. Eichling, and Lawrence G. Sharpe. "Central noradrenergic regulation of cerebral blood flow and vascular permeability." *Proceedings of the National Academy of Sciences* 72, no. 9 (1975): 3726-3730. https://doi.org/10.1073/pnas.72.9.3726

[41] Taqi, Muhammad A., Marc A. Lazzaro, Dhruvil J. Pandya, Aamir Badruddin, and Osama O. Zaidat. "Dissecting aneurysms of posterior cerebral artery: clinical presentation, angiographic findings, treatment, and outcome." *Frontiers in Neurology* 2 (2011): 38. https://doi.org/10.3389/fneur.2011.00038